journal

J. Am. Ceram. Soc., 90 [12] 3767–3772 (2007)
DOI: 10.1111/j.1551-2916.2007.02038.x

Preparation of Iron Phosphide Particles from an Aqueous Solvent of Oxygen-Contained Precursors Using Spray Pyrolysis

Kee Young Koo and Seung Bin Park†

Department of Chemical and Biomolecular Engineering, Korea Advanced Institute of Science and Technology, Daejeon 305-701, Korea

Iron phosphides were prepared by an economically feasible spray pyrolysis method, in which nontoxic and inexpensive precursors are used in an aqueous solution. The addition of NaCl to the precursor solution promoted crystal growth at a low temperature and helped to avoid sintering during posttreatment. The key conclusion is that the stoichiometry, shape, and size of the particles are related to the NaCl/Fe molar ratio and the posttreatment temperature. Below the melting temperature of NaCl, the shape and stoichiometry of the particles depended on the NaCl/Fe molar ratio, while above the melting temperature, they were dominated by the posttreatment temperature. Wire-like particles were formed at a NaCl/Fe molar ratio over 15.

I. Introduction

TRANSITION metal phosphides are considered to be one of the candidates for application as magnetic, optical, and electronic semiconductors, because physical properties are controlled by stoichiometry[1–5] and the shape and size[6] of phosphide particles. In particular, iron phosphides are one of the most important groups of transition metal phosphides due to their applications as low band gap semiconductor materials,[7] electrode materials,[8] catalysts,[9] magnetic storage media, and diluted magnetic semiconductors when doped with magnetic ions (V, Cr, Mn, Co, and Ni).[10,11] Previous works have demonstrated that the magnetic properties of iron phosphides are sensitive to their stoichiometry, size, and shape.[12,13]

Iron phosphides are synthesized by various conventional methods such as reduction of iron phosphate,[9,14,15] solvothermal process,[10,16] and thermal decomposition of metal–organic complexes.[11–13,17] Typically, these conventional methods require prolonged heat treatment at a high temperature [9,14,15] and cautious handling of toxic precursors and organic solvents such as trioctylphosphane (TOP), trioctylphosphine oxide (TOPO),[7,18–21] and triethylphosphine.[22] Moreover, these precursors are complex and expensive. It is difficult to control the stoichiometry of the final iron phosphides in these conventional preparation routes.

In this report, we propose an economically feasible method for preparing iron phosphides via spray pyrolysis at a low temperature using nontoxic and inexpensive precursors such as iron nitrate and ammonium phosphate. The dependence of the magnetic properties of iron phosphides on the stoichiometry and shape is reported. Spray pyrolysis is an aerosol process that produces solid particles via reactions of precursors within aerosol droplets.[23–25] The advantages of spray pyrolysis are availability of cheap and nontoxic precursors, controllability of composition, and the high purity of the products.[26–29]

Nevertheless, spray pyrolysis has never been used to prepare iron phosphides, because it is not commonly accepted that nonoxide particles are prepared from oxygen-contained precursors and processed under an oxygen-rich condition such as an aqueous solution. Another reason is that the residence time in the conventional spray pyrolysis is too short to produce crystalline nonoxide particles.[30,31] This means that a posttreatment step is required to produce fully crystallized and reduced particles. However, posttreatment makes the particles agglomerated and produces particles of irregular shape. To prevent the agglomeration of particles and improve the crystallization at a low temperature over short times, sodium chloride was added to the precursor solution before atomization. Xia *et al.*[32] reported that the addition of salt to the aqueous solution in the spray pyrolysis helped to keep the particles segregated inside a droplet and to produce nanosize particles.[33]

II. Experimental Procedure

(1) Solution Preparation

Iron(II) nitrate hexahydrate ($Fe(NO_3)_2 \cdot 6H_2O$, 98%, Junsei, Tokyo, Japan) and ammonium hydrogenphosphate ($(NH_4)_2 \cdot HPO_4$, 98%, Aldrich, St. Louis, MO) were used as precursors of iron and phosphorus, respectively. Nitric acid (HNO_3, Junsei, 60%–62%) was added to the precursor solution until a clear solution was obtained. The concentration of the Fe and P precursors was fixed at 0.3*M*, while the NaCl/Fe molar ratio was varied from 0 to 20. Sodium chloride (NaCl, Junsei, 99.5%) was used as the segregating agent.

(2) Spray Pyrolysis

A schematic diagram of the experimental apparatus for the spray pyrolysis system is shown in Fig. 1. In the conventional spray pyrolysis method, droplets are generated by an atomizer and transported into the furnace by a carrier gas. The particles are directly formed after the decomposition of precursors in a furnace-type reactor.[21,32] The H_2 (50% vol%)/N_2 mixed carrier gas flow rate was 1 L/min and the residence time in the tubular furnace-type reactor was 4–5 s. The particles produced were then posttreated at 600°–1000°C for 2–6 h under H_2 (20% vol%)/N_2 mixed gas (1 L/min) for further crystallization and reduction of iron phosphates within the particles. In salt-assisted spray pyrolysis, the salt (NaCl) was removed by washing with deionized water and then the particles were dried at room temperature.

(3) Characterization

The crystal structure and compositional homogeneity of the particles were examined by X-ray diffraction (XRD, Rigaku D/Max-β C, Tokyo, Japan, Cu$K\alpha$ radiation), and the lattice constants of Fe_2P were refined by a least-square method using the Lattice Constant Refinement Program of the Rigaku software. Energy-dispersive X-ray spectroscopy (EDS, EDAX,

T. Vanderah—contributing editor

Manuscript No. 22961. Received March 20, 2007; approved August 2, 2007.
This work was supported by Center for Ultramicrochemical Process Systems sponsored by KOSEF.
†Author to whom correspondence should be addressed. e-mail: SeungBinPark@kaist.ac.kr

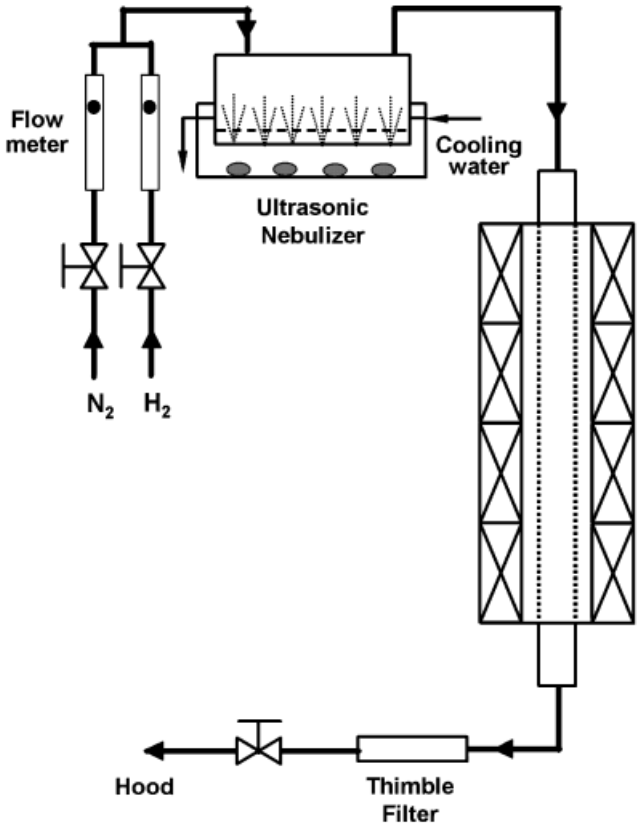

Fig. 1. Schematic diagram of the spray pyrolysis system.

Genesis, Mahwah, NJ) was performed to identify the elements present in the powder. The morphology and size of the particles were determined by scanning electron microscopy (SEM, Philips XL30SREG, Eindhoven, the Netherlands) and transmission electron microscopy (TEM, TECNAI F30 S-TWIN, FEI, Eindhoven, the Netherlands). The hysteresis curves (*M–H* curve) of the iron phosphides were obtained at room temperature using a vibrating sample magnetometer (VSM, RIKEN CENSHI VT-800, Tokyo, Japan). The temperature dependence of the magnetization curve (*M–T* curve) during zero-field-cooling (ZFC) and field-cooling (FC) procedures was examined by a Squid magnetometer (Quantum Design, MPMS-XL, San Diego, CA) between 5 and 400 K.

III. Results and Discussion

(1) Formation of Iron Phosphides by Conventional Spray Pyrolysis

In conventional spray pyrolysis, iron phosphides FeP and Fe_2P were formed after posttreatment at temperatures of 700°C and above. The XRD patterns of the iron phosphides prepared by spray pyrolysis are shown in Fig. 2. At 900° and 1000°C, the spray-pyrolyzed particles had an amorphous structure (Fig. 2(a)). After posttreatment at 700°C, FeP and $Fe_2P_2O_7$ (ferrous diphosphate) formed, with FeP only being present at 900°C and Fe_2P and FeP coexisting at 1000°C. EDS analysis was used to identify the elemental composition of the powders (Table I). This analysis demonstrated that iron, phosphorus, and oxygen are present in the particles, and that the atomic ratio of oxygen decreases with increasing posttreatment temperature and time. EDS data show that particles are composed of higher atomic percent of Fe and O. This is due to the fact that iron oxide and iron phosphate are present in the amorphous phase, which is not detected in XRD analysis. The XRD and EDS analysis results indicate that the particles require posttreatment for further crystallization and reduction of particles. The stoichiometry of iron and phosphorus depended on the posttreatment temperature and time. However, SEM images of the particles (Fig. 3) revealed severe agglomeration after posttreatment, which can be attributed to the sintering of particles.

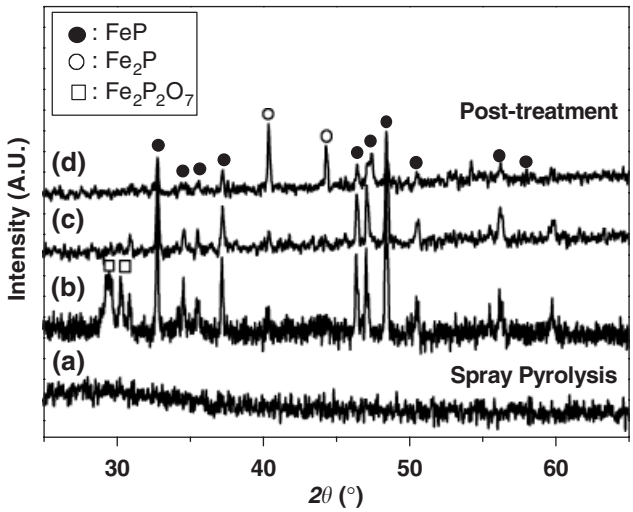

Fig. 2. X-ray diffraction patterns of particles prepared by conventional spray pyrolysis at (a) 900°C and then posttreated at (b) 700°C, (c) 900°C, or (d) 1000°C under 20% H_2/N_2 mixed gas for 2 h.

(2) Salt-Assisted Spray Pyrolysis: Effect of Salt Concentration on the Stoichiometry and Shape in Iron Phosphides

Addition of salt in the salt-assisted spray pyrolysis solves problems of conventional spray pyrolysis with regard to the agglomeration of particles and crystallization at a low temperature over short times during posttreatment. Figure 4 shows the XRD patterns of particles prepared with NaCl/Fe molar ratios of 5, 10, 15, and 20. At all NaCl/Fe molar ratios, Fe_2P was formed after posttreatment at 600°C for 6 h. However, Fe_2P and sodium iron phosphate coexisted at the NaCl/Fe molar ratio of 5. All XRD patterns of the Fe_2P phase can be indexed to a hexagonal structure with the space group *P*-62*m* (PDF: 85–1727), and the refined lattice constants are $a = 5.8664$ Å and $c = 3.4624$ Å. We suggest that salt plays the role of a matrix in keeping the intermediates of Fe_2P particles apart above an NaCl/Fe molar ratio of 10, whereas at a low salt concentration, the crystallites remain close to each other and agglomerate.[33] SEM pictures (Fig. 5) of the particles prepared with various NaCl/Fe molar ratios show that they are wire-like and spherical in shape. These images show that, as the salt concentration is increased, the particle size decreases and wire-like particles are formed. The wire-like particles were examined further by means of TEM. TEM images show that a wire-like Fe_2P with a high aspect ratio was formed (Fig. 6(a)). Select area electron diffractions (SAED) confirm that Fe_2P nanowire is a single crystal that grows perpendicular to the (001) plane of a basal plane of a hexagonal system (inset of Fig. 6(a)). Fe_2P nanowire shows (001), (101), and (100) reflection

Table I. EDS Data of Particles Prepared by Conventional Spray Pyrolysis and then Posttreated at Various Temperatures

Spray pyrolysis	Posttreatment	Iron (at.%)	Phosphorus (at.%)	Oxygen (at.%)
900°C	—	23	20	57
	700°C, 2 h	35	30	35
	900°C, 2 h	54	37	9
	900°C, 6 h	62	38	0
	1000°C, 2 h	68	33	0
1000°C	—	21	20	59

EDS, energy-dispersive X-ray spectroscopy.

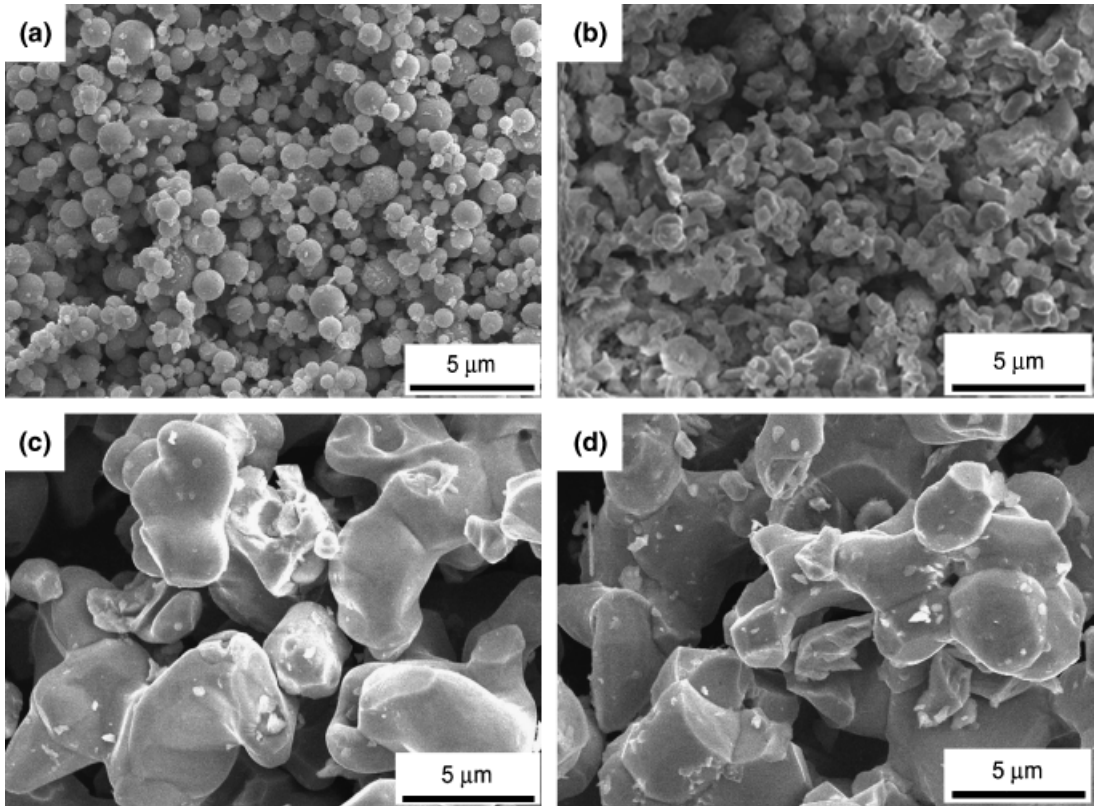

Fig. 3. Scanning electron microscopy images of particles prepared by conventional spray pyrolysis at (a) 900°C and posttreated at (b) 700°C, (c) 900°C, or (d) 1000°C under 20% H_2/N_2 mixed gas for 2 h.

characteristics of the [010] orientation of an Fe_2P hexagonal structure ($a = 5.867$ Å, $c = 3.458$ Å, PDF: 85–1727). High-resolution transmission electron microscopy image of particles shows that the lattice fringe distances are 3.5 and 5.1 Å, consistent with Fe_2P interplanar spacing ($d_{001} = 3.4581$ Å, $d_{100} = 5.0813$ Å) (Fig. 6(b)). EDS analysis reveals that the stoichiometric ratios of iron and phosphorus are in the range of 1.5:1–2:1 in the wire-like particles (Fig. 7). It seems likely that an excess amount of phosphorus exists in the amorphous phase, and that oxygen is present due to surface oxidation. On the other hand, sodium remains in spherical particles and slightly more oxygen exists. From the EDS data, we found that the unconfirmed amorphous phase was sodium iron phosphate. We were unable to remove sodium iron phosphate selectively by washing.

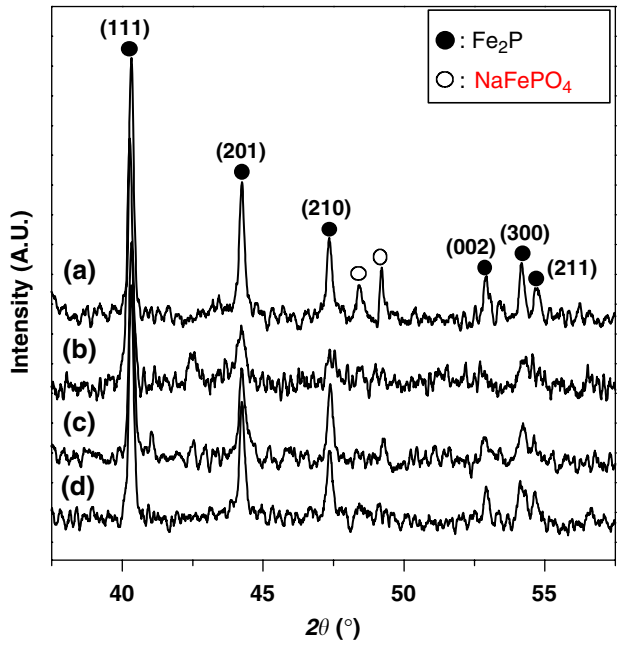

Fig. 4. X-ray diffraction patterns of particles prepared by salt-assisted spray pyrolysis at 700°C with various NaCl/Fe molar ratios of (a) 5, (b) 10, (c) 15, or (d) 20, and then posttreated at 600°C under 20% H_2/N_2 mixed gas for 6 h.

(3) Magnetic Property: Comparison of Magnetic Property Due to Shape Anisotropy and Stoichiometry

The magnetic property of iron phosphides was investigated by changing the salt concentration and posttreatment temperature: the magnetic properties were measured by means of VSM and SQUID analysis. We confirmed that the salt concentration affected both the stoichiometry and crystalline growth in the particles and that wire-like particles were formed and the volumetric ratio of wire-like particles increased as the salt concentration increased in SEM images (Fig. 5). Hence, we expected that the magnetization of particles during ZFC and FC processes and transition temperature depended on the transformation of particle shape and the decrease of particle size owing to effect of the addition of salt. However, diamagnetization was observed, which we ascribe to the compositional inhomogeneity caused by the presence of sodium iron phosphate.

In the present study, we observe that Fe_2P shows magnetic hysteresis at room temperature. It is known that Fe_2P exhibits a first-order ferromagnetic–paramagnetic transition between −58° and −7°C.[12,13] We presume that the magnetic hysteresis arises from the formation of iron-rich phosphides (Fe_3P) or iron oxide with a structure that is an amorphous phase, whose detection is not possible by XRD. Figure 8 shows the XRD patterns of particles posttreated at various temperatures. We identified Fe_2P and Fe_3P coexisting after posttreatment at 800° or 900°C, whereas only Fe_2P existed after posttreatment at

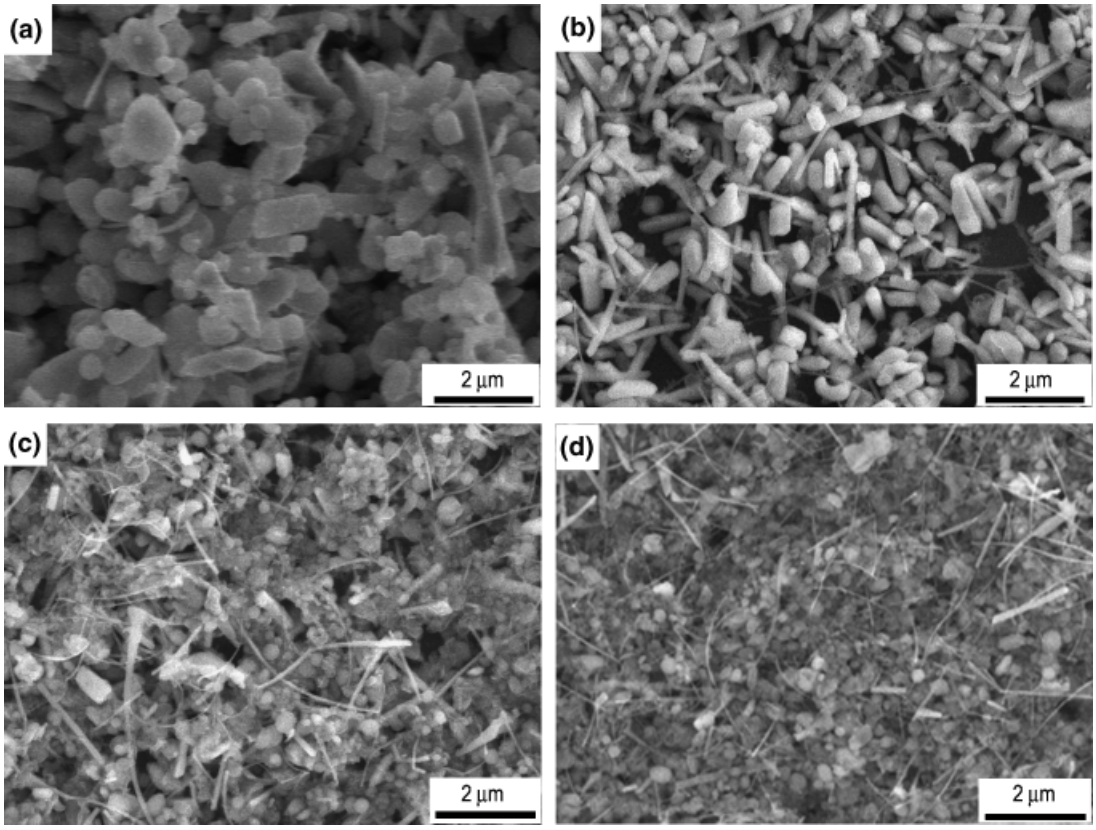

Fig. 5. Scanning electron microscopy images of particles prepared by salt-assisted spray pyrolysis at various NaCl/Fe molar ratios, (a) 5, (b) 10, (c) 15, or (d) 20, and then post treated at 600°C for 6 h.

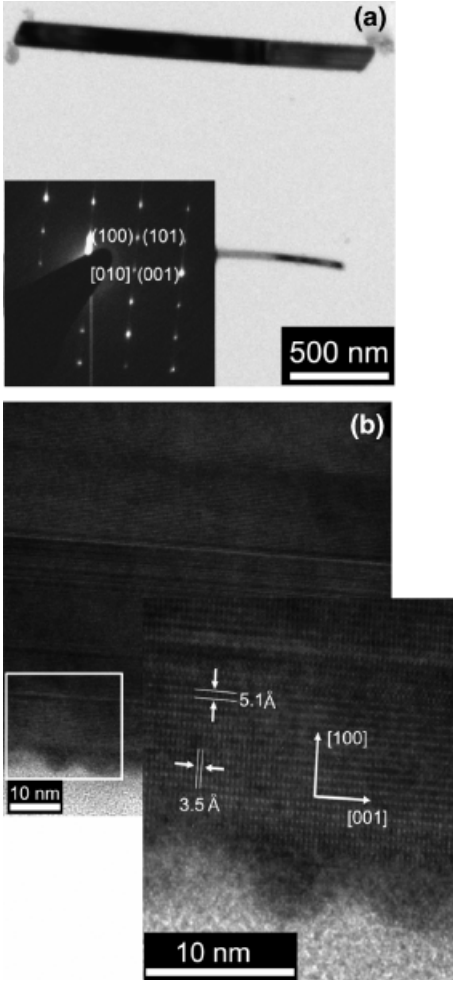

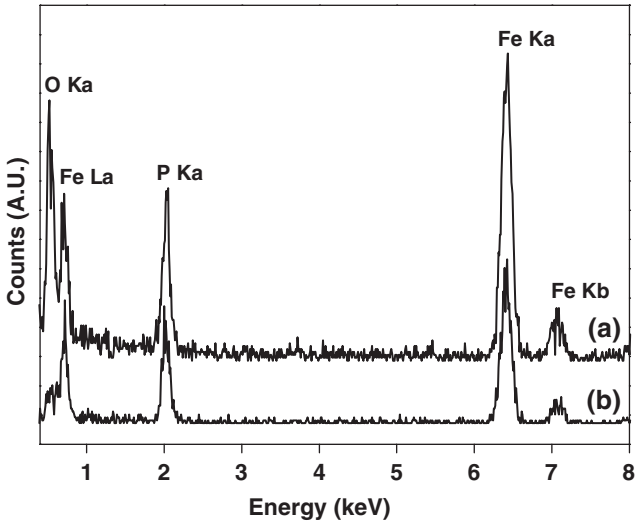

Fig. 7. Energy Dispersive X-ray spectroscopy data of wire-like particles prepared at a NaCl/Fe molar ratio of 20. On the (a) surface of particles, the actual atomic composition is Fe 37%, P 15%, and O 48%, whereas Fe 60%, P 40%, and O 0% at the (b) center.

1000°C. In Table II, the EDS result shows that no sodium is left in the particle at the posttreatment temperature of 1000°C. Some iron component exists as pure iron. This result is consistent with Park *et al.*'s report in which they claimed that there

Fig. 6. (a) Bright field image (inset: select area electron diffraction pattern) and (b) high-resolution transmission electron microscopy image of Fe_2P particles prepared at 700°C using a NaCl/Fe molar ratio of 20 and then posttreated at 600°C for 6 h.

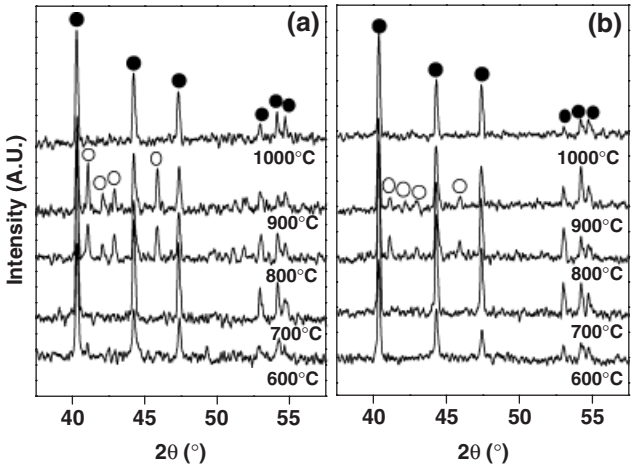

Fig. 8. X-ray diffraction patterns of particles prepared by SASP with NaCl/Fe molar ratios of (a) 15 and (b) 20, posttreated at 600° to 1000°C. (●) Fe_2P, (○) Fe_3P.

Table II. EDS Data of Particles Prepared by Salt-Assisted Spray Pyrolysis and then Posttreated at 1000°C

NaCl/Fe molar ratio	Iron (at.%)	Phosphorus (at.%)	Oxygen (at.%)
15	76	24	0
20	74	26	0

EDS, energy-dispersive X-ray spectroscopy.

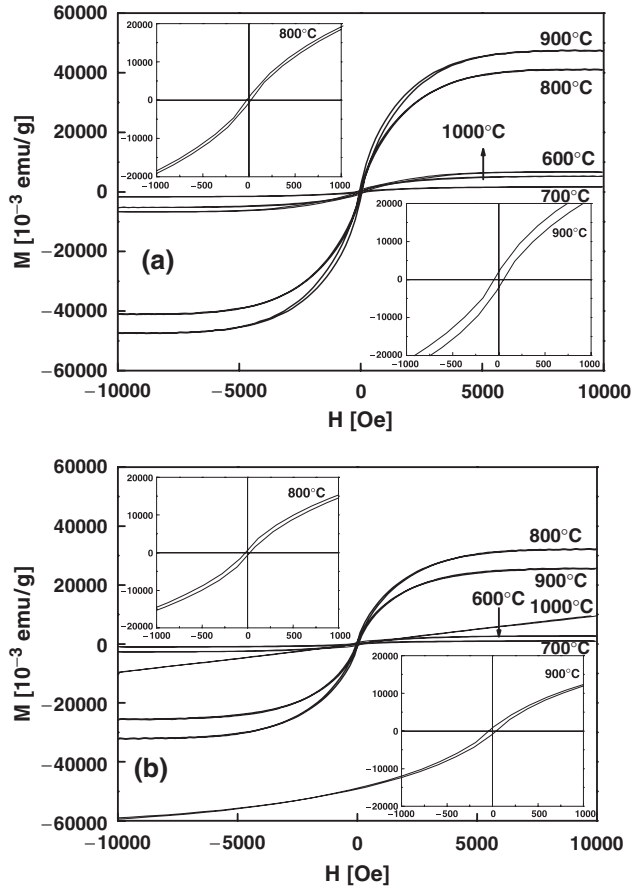

Fig. 9. Magnetization versus applied field (M–H curve) for particles prepared by SASP with NaCl/Fe molar ratios of (a) 15 and (b) 20, posttreated at 600°, 700°, 800°, 900°, and 1000°C.

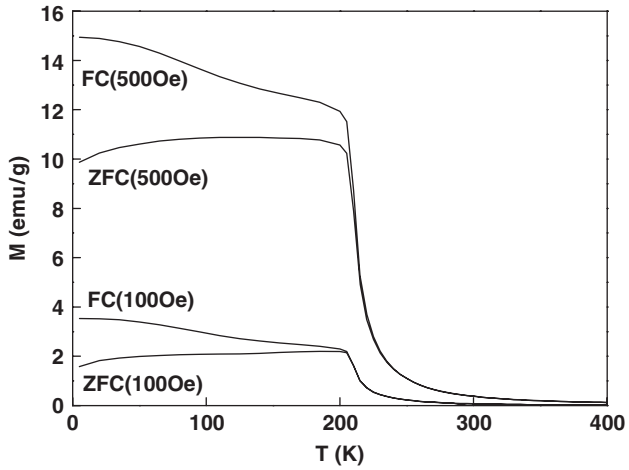

Fig. 10. Magnetization versus temperature for Fe_2P prepared by SASP with a NaCl/Fe molar ratio of 20 and posttreated at 1000°C for 6 h.

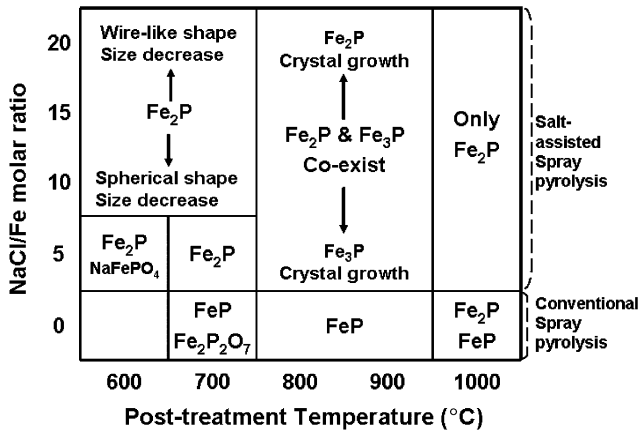

Fig. 11. Shape and stoichiometry of iron phosphides prepared by spray pyrolysis.

exists a small fraction of pure iron or other Fe-rich phase in the amorphous phase.[21] The M–H curve (Fig. 9) shows that the change in the composition of iron phosphide with increasing posttreatment temperature influenced the magnetic behavior of the particles. The saturated magnetization (M_s) value is the highest for the systems posttreated at 800° or 900°C, in which Fe_2P and Fe_3P coexisted. The M–T curve of Fe_2P formed at 1000°C, obtained by means of SQUID analysis, shows a blocking temperature close to the bulk ferromagnetic transition temperature of 215 K (Fig. 10). There is no characteristic behavior of pure iron or Fe_3P in the SQUID measurement.

Combining the results of EDS (Table II), XRD (Fig. 8), and SQUID measurement (Fig. 10), we conclude that Fe_2P is the major phase at 1000°C of posttreatment temperature.

IV. Conclusions

Iron phosphide particles were prepared by spray pyrolysis from nontoxic and inexpensive precursors in an aqueous solution. In conventional spray pyrolysis, the particles were severely agglomerated during posttreatment. In salt-assisted spray pyrolysis, by contrast, homogeneous and isolated Fe_2P wire-like particles were formed at a low temperature (600°C).

Two key variables affecting shape and stoichiometry were identified, and the results were summarized on a plot of NaCl/Fe molar ratio versus posttreatment temperature as shown in Fig. 11. When salt was not added (conventional spray pyrolysis),

homogeneous FeP particles were formed above 800°C, while the formation of Fe_2P required a high temperature of 1000°C. However, Fe_2P particles were formed at a low temperature of 600°C when salt was added (salt-assisted spray pyrolysis).

As the salt concentration was increased at a fixed temperature of 600°C, wire-like Fe_2P particles were formed and the size of the particles decreased. Fe_2P and Fe_3P coexisted after posttreatment at 800° or 900°C, whereas only Fe_2P existed after posttreatment at 1000°C. Unexpected magnetic hysteresis at room temperature was considered to be an evidence of formation of an iron-rich amorphous phase (Fe_3P).

In summary, below the melting temperature of the NaCl ($T <$ 800°C), the stoichiometry and shape of iron phosphides depended on the NaCl concentration, whereas above the melting temperature of NaCl, the posttreatment temperature determined the stoichiometry and shape of iron phosphides.

Acknowledgments

The authors thank the National Nanofab Center for TEM examination and Korea Basic Science Institute for SQUID measurement.

References

[1]S. C. Perera, G. Tsoi, L. E. Wenger, and S. L. Brock, "Synthesis of MnP Nanocrystals by Treatment of Metal Carbonyl Complexes with Phosphines: A New, Versatile Route to Nanoscale Transition Metal Phosphides," *J. Am. Chem. Soc.*, **125**, 13960–1 (2003).

[2]Y. Gu, L. Chen, Y. Qian, and H. Gu, "Solvothermal Synthesis of Titanium Phosphides Via Sodium Co-Reduction of PCl_3 and $TiCl_4$," *J. Mater. Sci. Lett.*, **22**, 1463–4 (2003).

[3]J. Nowacki, "Structure and Properties of Thin Iron Phosphide Films on Carburised Layers," *Surf. Coat. Technol.*, **180–181**, 566–9 (2004).

[4]Yu. H. Budnikova, D. I. Tazeev, B. A. Trofimov, and O. G. Sinyashin, "Electrosynthesis of Nickel Phosphides on the Basis of White Phosphorus," *Electrochem. Comm.*, **6**, 700–2 (2004).

[5]B. Mauvernay, M.-L. Doublet, and L. Monconduit, "Redox Mechanism in the Binary Transition Metal Phosphide Cu_3P," *J. Phys. Chem. Solid*, **67**, 1252–7 (2006).

[6]K. A. Gregg, S. C. Perera, G. Lawes, S. Shinozaki, and S. L. Brock, "Controlled Synthesis of MnP Nanorods: Effect of Shape Anisotropy on Magnetization," *Chem. Mater.*, **18**, 879–86 (2006).

[7]J.-H. Chen, M.-F. Tai, and K.-M. Chi, "Catalytic Synthesis, Characterization and Magnetic Properties of Iron Phosphide Nanowires," *J. Mater. Chem.*, **14**, 296–8 (2004).

[8]S. Boyanov, J. Bernardi, F. Gillot, L. Dupont, M. Womes, J. M. Tarascon, L. Monoconduit, and M. L. Doublet, "FeP: Another Attractive Anode for the Li-Ion Battery Enlisting a Reversible Two-Step Insertion/Conversion Process," *Chem. Mater.*, **18**, 3531–8 (2006).

[9]S. T. Oyama, "Novel Catalysts for Advanced Hydroprocessing: Transition Metal Phosphides," *J. Catal.*, **216**, 343–52 (2003).

[10]F. Luo, H. L. Su, W. Song, Z. M. Wang, Z. G. Yan, and C. H. Yan, "Magnetic and Magnetotransport Properties of Fe_2P Nanocrystallites *via* a Solvothermal Route," *J. Mater. Chem.*, **14**, 111–5 (2004).

[11]C. M. Lukehart, S. B. Milne, S. R. Stock, R. D. Shull, and J. E. Wittig, "Nanocomposites Containing Nanoclusters of Fe_2P or γ-Fe_2O_3," *Mater. Sci. Eng. A*, **204**, 176–80 (1995).

[12]R. Wäppling, L. Häggström, S. Rundqvist, and E. Karlsson, "Mössbauer Study of Phosphides Containing Iron," *J. Solid State Chem.*, **3**, 276–92 (1971).

[13]S. L. Brock, S. C. Perera, and K. L. Stamm, "Chemical Routes for Production of Transition-Metal Phosphides on the Nanoscale: Implications for Advanced Magnetic and Catalytic Materials," *Chem. Eur. J.*, **10**, 3364–71 (2004).

[14]K. L. Stamm, J. C. Garno, G. Liu, and S. L. Brock, "A General Methodology for the Synthesis of Transition Metal Pnictide Nanoparticles from Pnictate Precursors and Its Application to Iron–Phosphorus Phases," *J. Am. Chem. Soc.*, **125**, 4038–9 (2003).

[15]J. Gopalakrishnan, S. Pandey, and K. K. Rangan, "Convenient Route for the Synthesis of Transition-Metal Pnictides by Direct Reduction of Phosphate, Arsenate, and Antimonate Precursors," *Chem. Mater.*, **9**, 2113–6 (1997).

[16]G. Yunle, G. Fan, Q. Yitai, Z. Huagui, and Y. Ziping, "A Solvothermal Synthesis of Ultra-Fine Iron Phosphide," *Mater. Res. Bull.*, **37**, 1101–5 (2002).

[17]C. M. Lukehart, S. B. Milne, and S. R. Stock, "Formation of Crystalline Nanoclusters of Fe_2P, RuP, Co_2P, Rh_2P, Ni_2P, Pd_5P_2, or PtP_2 in a Silica Xerogel Matrix from Single-Source Molecular Precursors," *Chem. Mater.*, **10**, 903–8 (1998).

[18]S. C. Perera, P. S. Fodor, G. M. Tsoi, L. E. Wenger, and S. L. Brock, "Application of De-Silylation Strategies to the Preparation of Transition Metal Pnictide Nanocrystals: The Case of FeP," *Chem. Mater.*, **15**, 4034–8 (2003).

[19]C. G. Hu, Y. Li, J. P. Liu, Y. Y. Zhang, G. Bao, B. Buchine, and Z. L. Wang, "Sonochemical Synthesis of Ferromagnetic Core-Shell Fe_3O_4–FeP Nanoparticles and FeP Nanoshells," *Chem. Phys. Lett.*, **428**, 343–7 (2006).

[20]C. Qian, F. Kim, L. Ma, F. Tsui, P. Yang, and J. Liu, "Solution-Phase Synthesis of Single-Crystalline Iron Phosphide Nanorods/Nanowires," *J. Am. Chem. Soc.*, **126**, 1195–8 (2004).

[21]J. Park, B. Koo, Y. Hwang, C. Bae, K. An, J.-G. Park, H. M. Park, and T. Hyeon, "Novel Synthesis of Magnetic Fe_2P Nanorods from Thermal Decomposition of Continuously Delivered Precursors Using a Syringe Pump," *Angew. Chem. Int. Ed.*, **43**, 2282–5 (2004).

[22]J. D. Sweet and D. J. Casadonte Jr., "Sonochemical Synthesis of Iron Phosphide," *Ultrason. Sonochem.*, **8**, 97–101 (2001).

[23]T. T. Kodas and M. J. Hampden-Smith, *Aerosol Processing of Materials*, pp. 11–3. Wiley-VCH, New York, 1999.

[24]G. L. Messing, S.-C. Zhang, and G. V. Jayanthi, "Ceramic Powder Synthesis by Spray Pyrolysis," *J. Am. Ceram. Soc.*, **76**, 2707–26 (1993).

[25]Y. C. Kang, Y. S. Chung, and S. B. Park, "Preparation of YAG: Europium Red Phosphors by Spray Pyrolysis Using a Filter-Expansion Aerosol Generator," *J. Am. Ceram. Soc.*, **82**, 2056–60 (1999).

[26]I. Colbeck and Y. Kamlag, "Preparation of Fine Particles by Spray Pyrolysis," *J. Aerosol. Sci.*, **27**, S395–6 (1996).

[27]Y. C. Kang, H. S. Roh, and S. B. Park, "Sodium Carbonate Flux Effects on the Luminescence Characteristics of $(Y_{0.5}Gd_{0.5})_2O_3$: Eu Phosphor Particles Prepared by Spray Pyrolysis," *J. Am. Ceram. Soc.*, **84**, 447–9 (2001).

[28]W. Nimmo, N. J. Ali, R. M. Brydson, C. Calvert, E. Hampartsoumian, D. Hind, and S. J. Milne, "Formation of Lead Zirconate Titanate Powders by Spray Pyrolysis," *J. Am. Ceram. Soc.*, **86**, 1474–80 (2003).

[29]Y. L. Song, S. C. Tsai, C. Y. Chen, T. K. Tseng, C. S. Tsai, J. W. Chen, and Y. D. Yao, "Ultrasonic Spray Pyrolysis for Synthesis of Spherical Zirconia Particles," *J. Am. Ceram. Soc.*, **87**, 1864–71 (2004).

[30]D. A. Lindquist, T. T. Kodas, D. M. Smith, X. Xiu, S. L. Hietala, and R. T. Paine, "Boron Nitride Powders Formed by Aerosol Decomposition of Poly(borazinylamine) Solutions," *J. Am. Ceram. Soc.*, **74**, 1326–8 (1991).

[31]M. Nyman, J. Caruso, and M. J. Hampden-Smith, "Comparison of Solid-State and Spray-Pyrolysis Synthesis of Yttrium Aluminate Powders," *J. Am. Ceram. Soc.*, **80**, 1231–8 (1997).

[32]B. Xia, I. W. Lenggoro, and K. Okuyama, "Novel Route to Nanoparticle Synthesis by Salt-Assisted Aerosol Decomposition," *Adv. Mater.*, **13**, 1579–82 (2001).

[33]Y. Itoh, M. Abdullah, and K. Okuyama, "Direct Preparation of Nonagglomerated Indium Tin Oxide Nanoparticles Using Various Spray Pyrolysis Methods," *J. Mater. Res.*, **19**, 1077–86 (2004). □